Electronic Supporting Information (ESI†)

for

Remarkable visible light-triggered cytotoxicity of mitochondria targeting mixed-ligand cobalt(III) complexes of curcumin and phenanthroline bases binding to human serum albumin

Tukki Sarkar,[a] Samya Banerjee*[b] and Akhtar Hussain*[a]

[a] *Department of Chemistry, Handique Girls' College, Guwahati-781001, Assam, India. [E-mail: akhtariisc@gmail.com; Tel: +91-36-12543793 for general correspondence].*

[b] *Department of Inorganic and Physical Chemistry, Indian Institute of Science, Bangalore-560 012, India. [E-mail: samya@ipc.iisc.ernet.in; Tel: +91-80-22932240].*

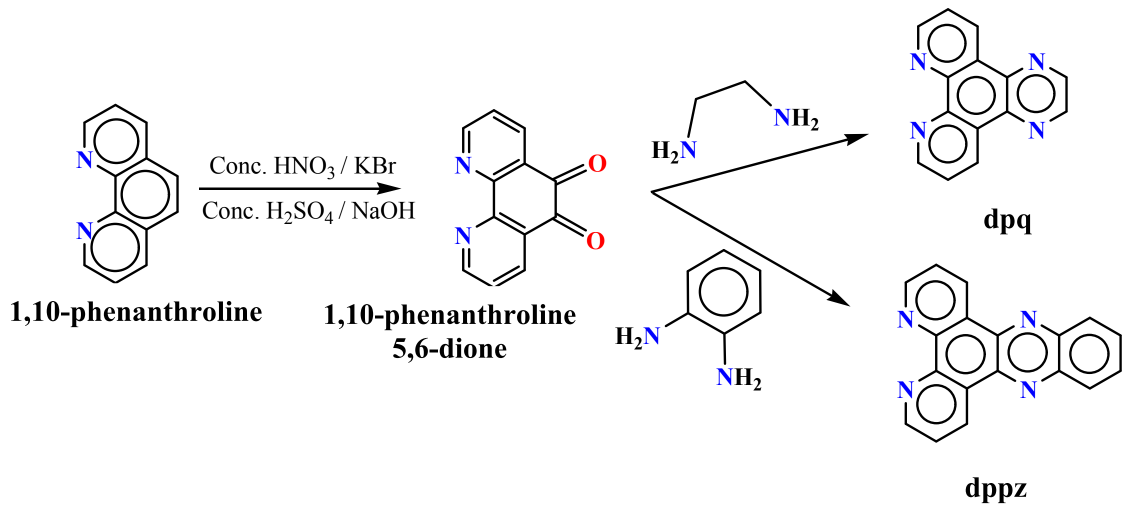

Figure S1. Schematic representation showing the synthetic route to dpq and dppz ligands.

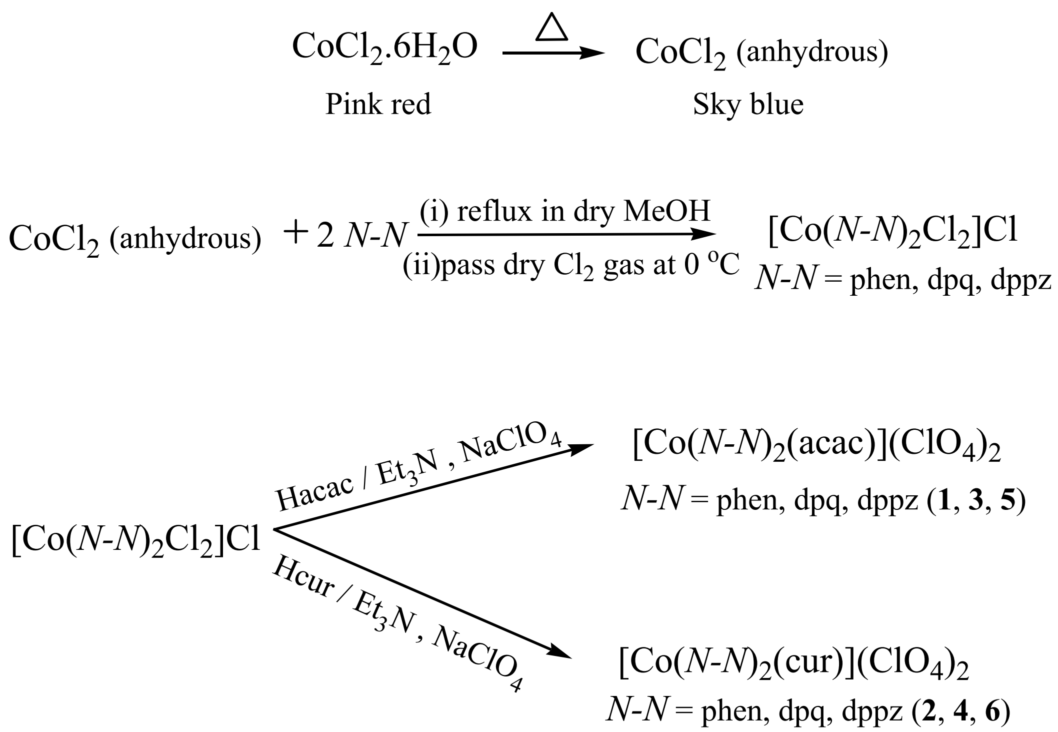

Figure S2. A generalized reaction scheme showing the syntheses of complexes **1–6**.

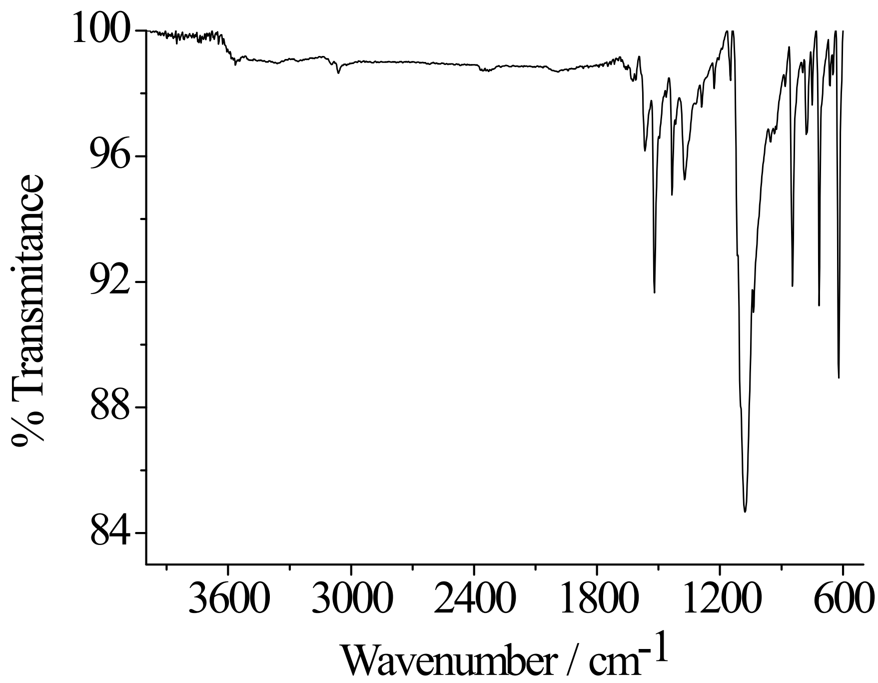

Figure S3. The IR spectrum of $[Co(phen)_2(acac)](ClO_4)_2$ (**1**).

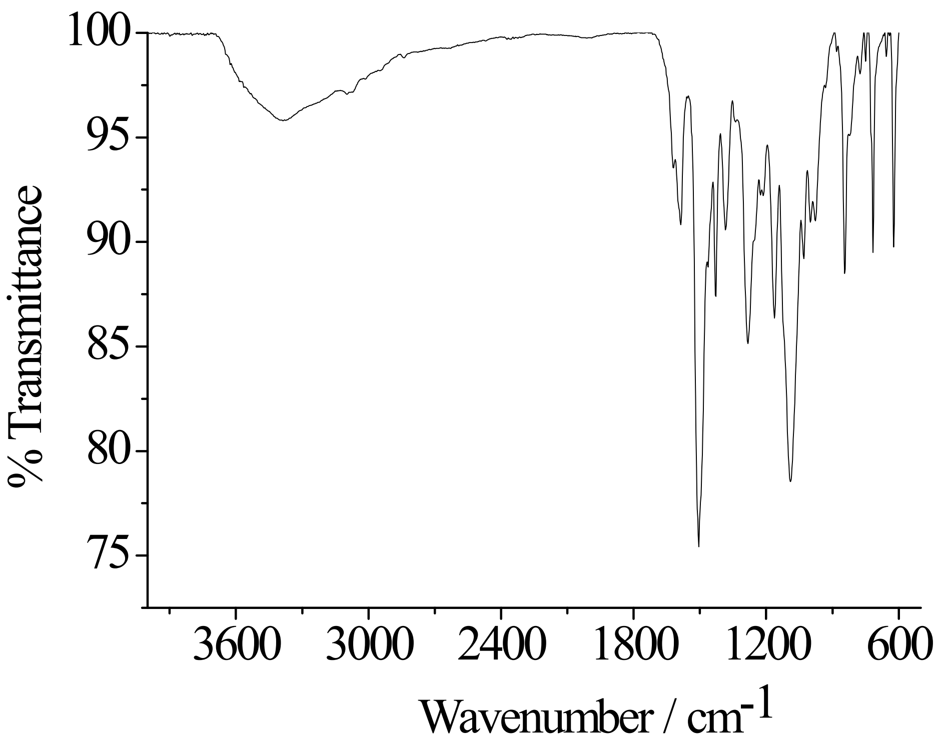

Figure S4. The IR spectrum of $[Co(phen)_2(cur)](ClO_4)_2$ (**2**).

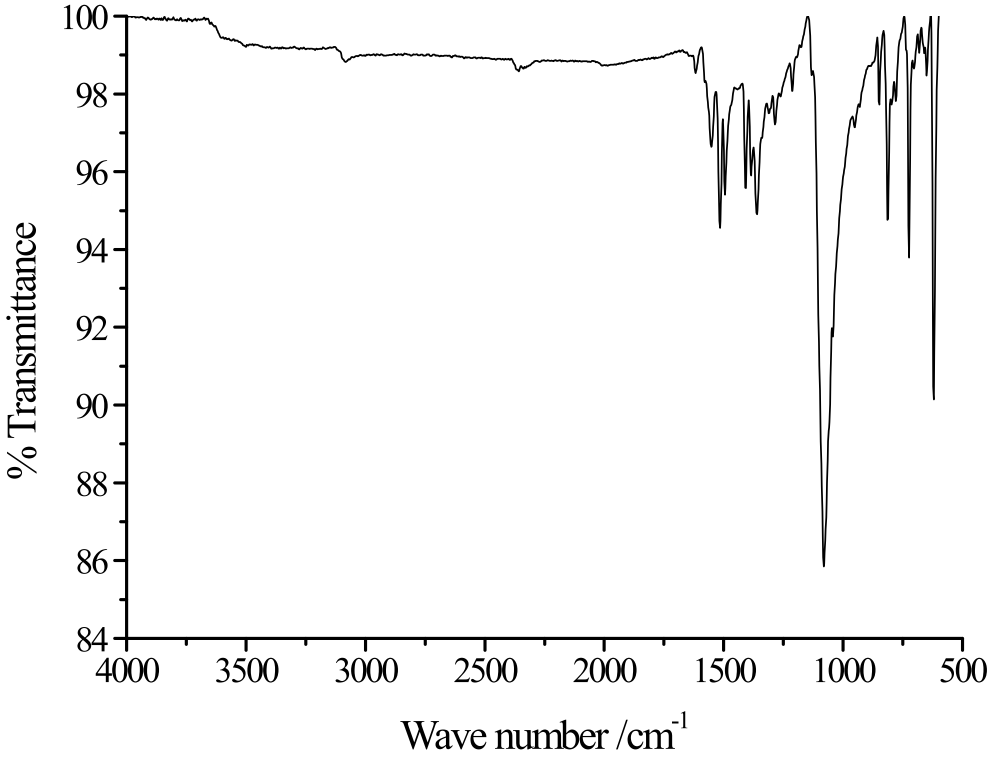

Figure S5. The IR spectrum of $[Co(dpq)_2(acac)](ClO_4)_2$ (**3**).

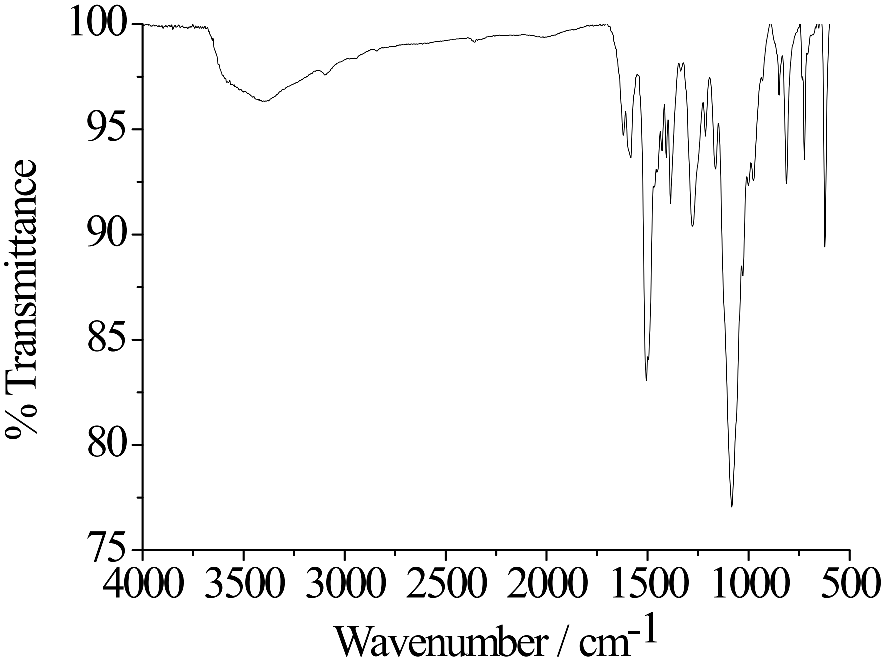

Figure S6. The IR spectrum of $[Co(dpq)_2(cur)](ClO_4)_2$ (**4**)

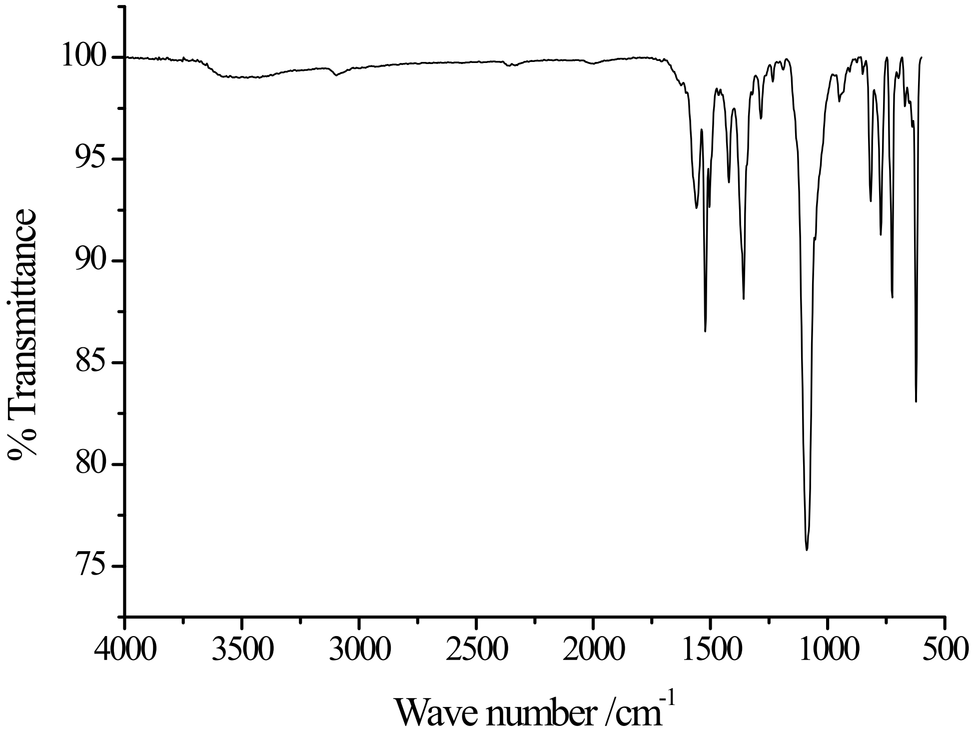

Figure S7. The IR spectrum of $[Co(dppz)_2(acac)](ClO_4)_2$ (**5**).

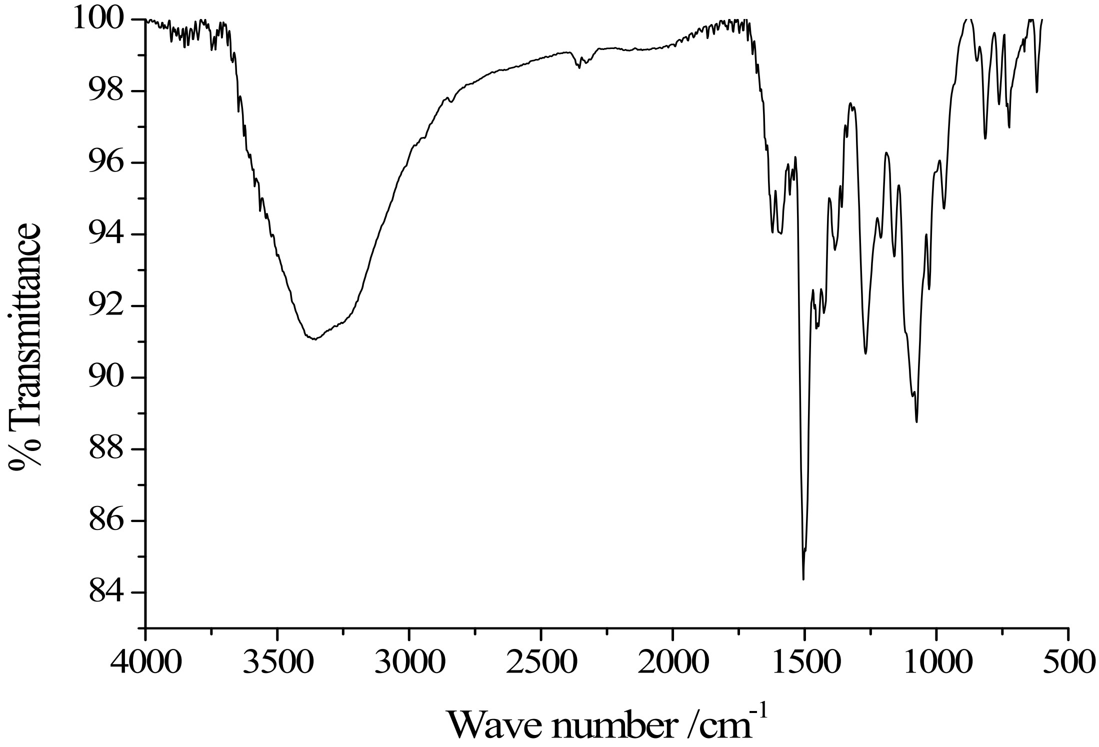

Figure S8. The IR spectrum of $[Co(dppz)_2(cur)](ClO_4)_2$ (**6**).

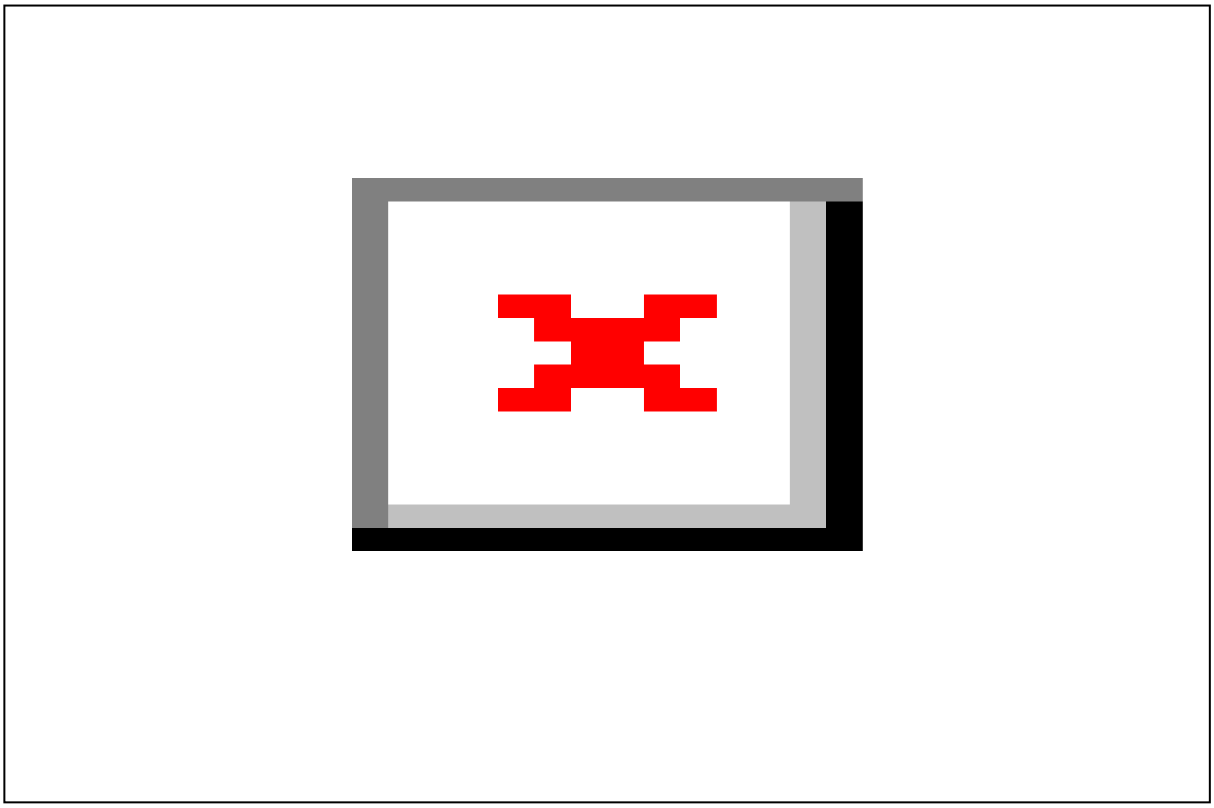

Figure S9. The ESI-MS spectrum of $[Co(phen)_2(cur)](ClO_4)_2$ (**2**) in 5% aqueous acetonitrile showing the $[M\text{-}2ClO_4^-]^{2+}$ peak.

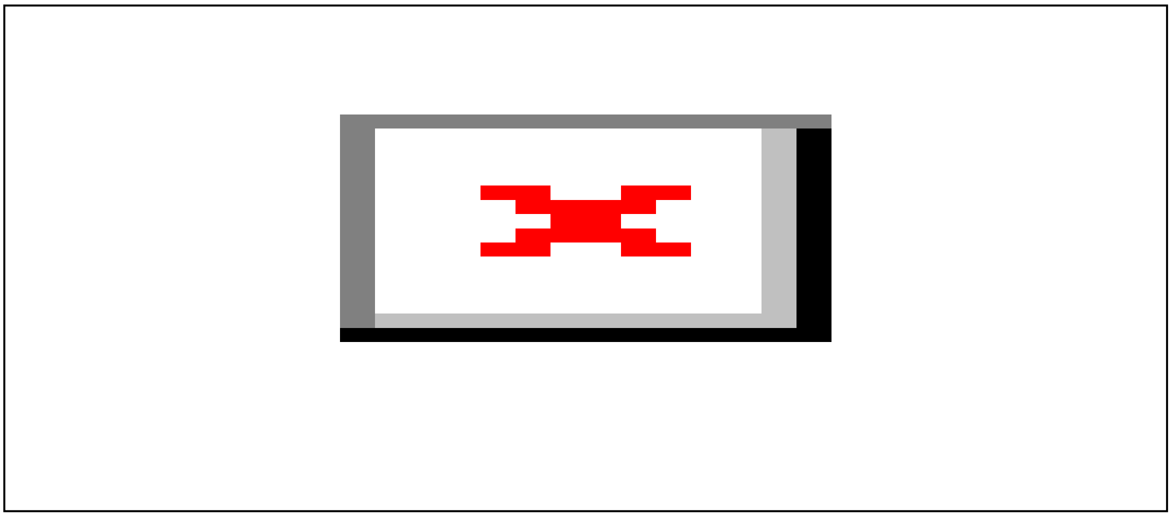

Figure S10. The isotopic distribution pattern for the $[M-2ClO_4^-]^{2+}$ peak of $[Co(phen)_2(cur)](ClO_4)_2$ (**2**) in the ESI-MS spectrum shown in Figure S9.

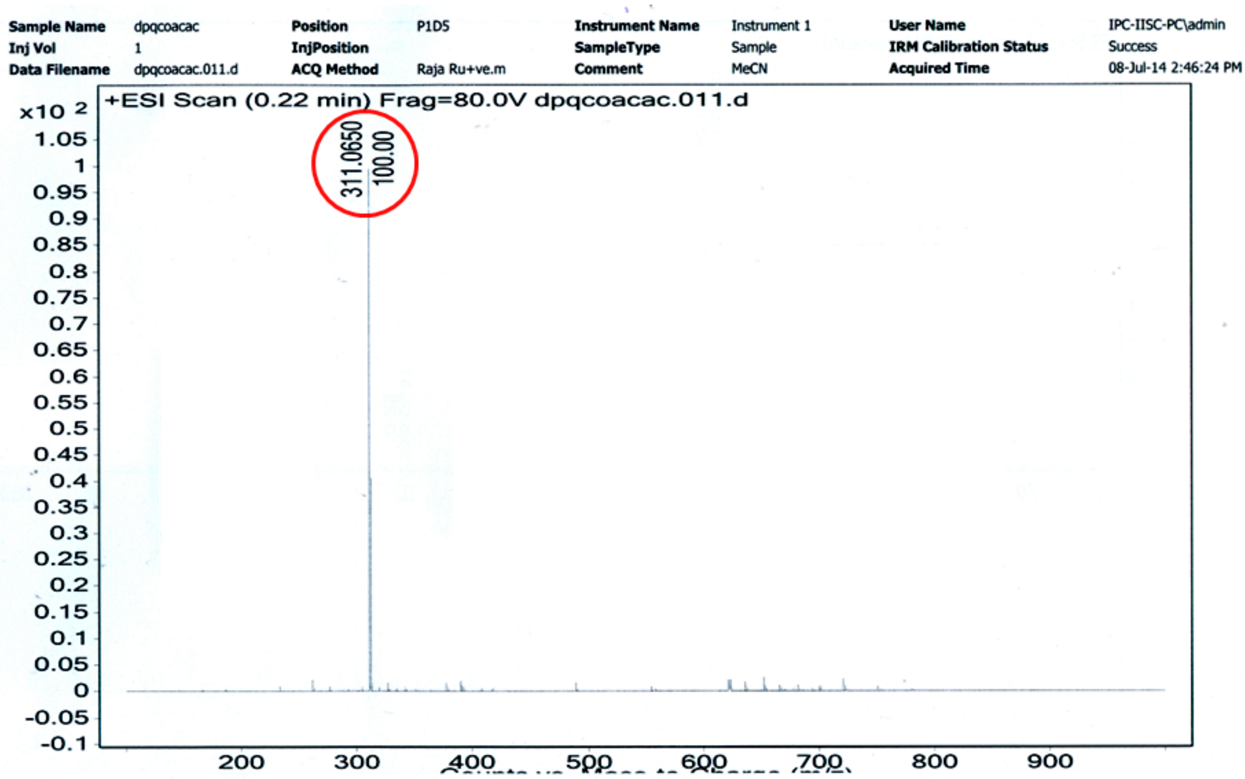

Figure S11. The ESI-MS spectrum of $[Co(dpq)_2(acac)](ClO_4)_2$ (**3**) in 5% aqueous acetonitrile showing the $[M\text{-}2ClO_4^-]^{2+}$ peak.

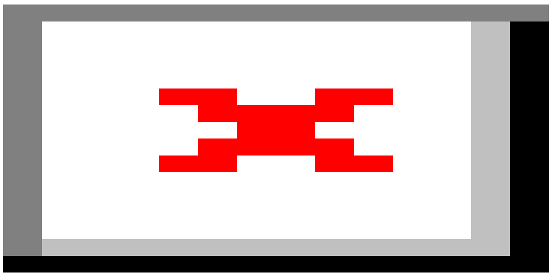

Figure S12. The isotopic distribution pattern for the $[M\text{-}2ClO_4^-]^{2+}$ peak of $[Co(dpq)_2(acac)](ClO_4)_2$ (**3**) in the ESI-MS spectrum shown in Figure S11.

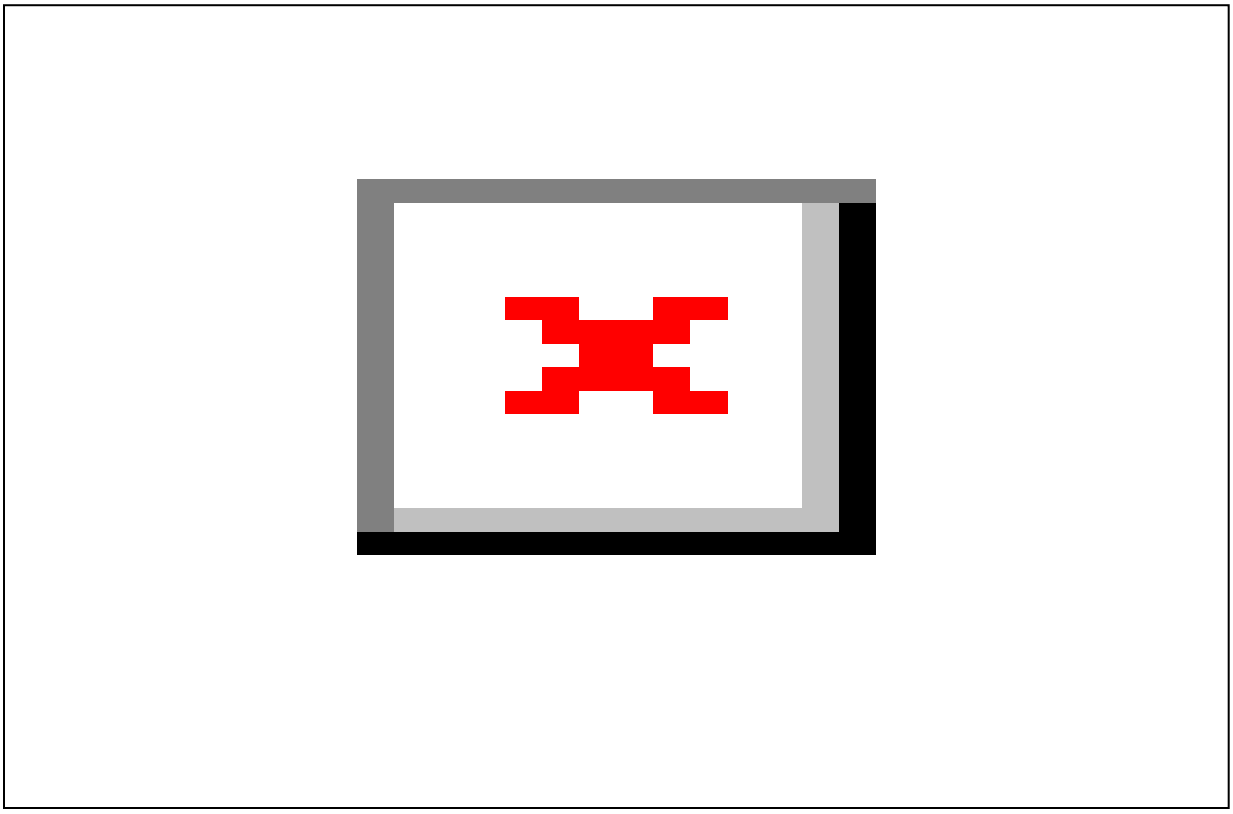

Figure S13. The ESI-MS spectrum of $[Co(dpq)_2(cur)](ClO_4)_2$ (**4**) in 5% aqueous acetonitrile showing the $[M\text{-}2ClO_4^-]^{2+}$ peak.

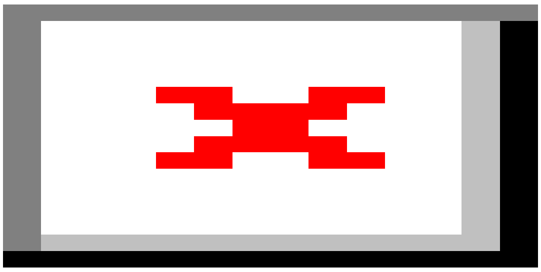

Figure S14. The isotopic distribution pattern for the $[M\text{-}2ClO_4^-]^{2+}$ peak of $[Co(dpq)_2(cur)](ClO_4)_2$ (**4**) in the ESI-MS spectrum shown in Figure S13.

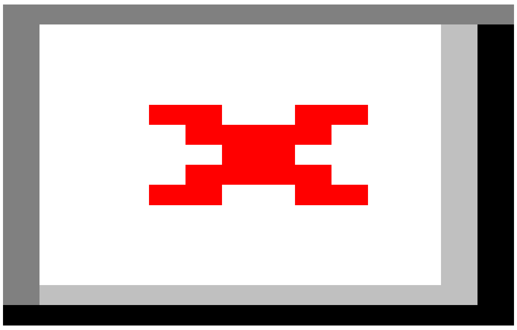

Figure S15. The ESI-MS spectrum of $[Co(dppz)_2(acac)](ClO_4)_2$ (**5**) in 5% aqueous acetonitrile showing the $[M\text{-}2ClO_4^-]^{2+}$ peak.

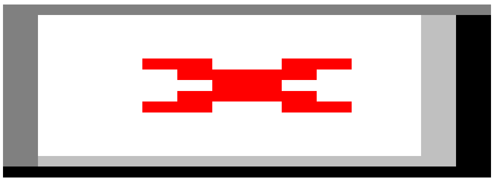

Figure S16. The isotopic distribution pattern for the $[M\text{-}2ClO_4^-]^{2+}$ peak of $[Co(dppz)_2(acac)](ClO_4)_2$ (**5**) in the ESI-MS spectrum shown in Figure S15.

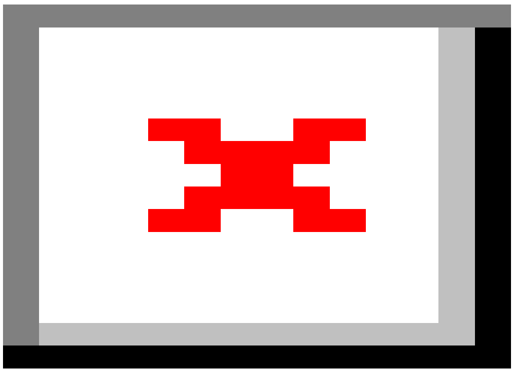

Figure S17. The ESI-MS spectrum of $[Co(dppz)_2(cur)](ClO_4)_2$ (**6**) in 5% aqueous acetonitrile showing the $[M-2ClO_4^-]^{2+}$ peak.

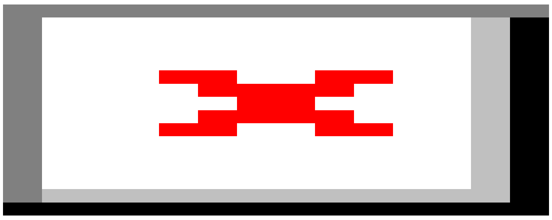

Figure S18. The isotopic distribution pattern for the $[M\text{-}2ClO_4^-]^{2+}$ peak of $[Co(dppz)_2(cur)](ClO_4)_2$ (**6**) in the ESI-MS spectrum shown in Figure S17.

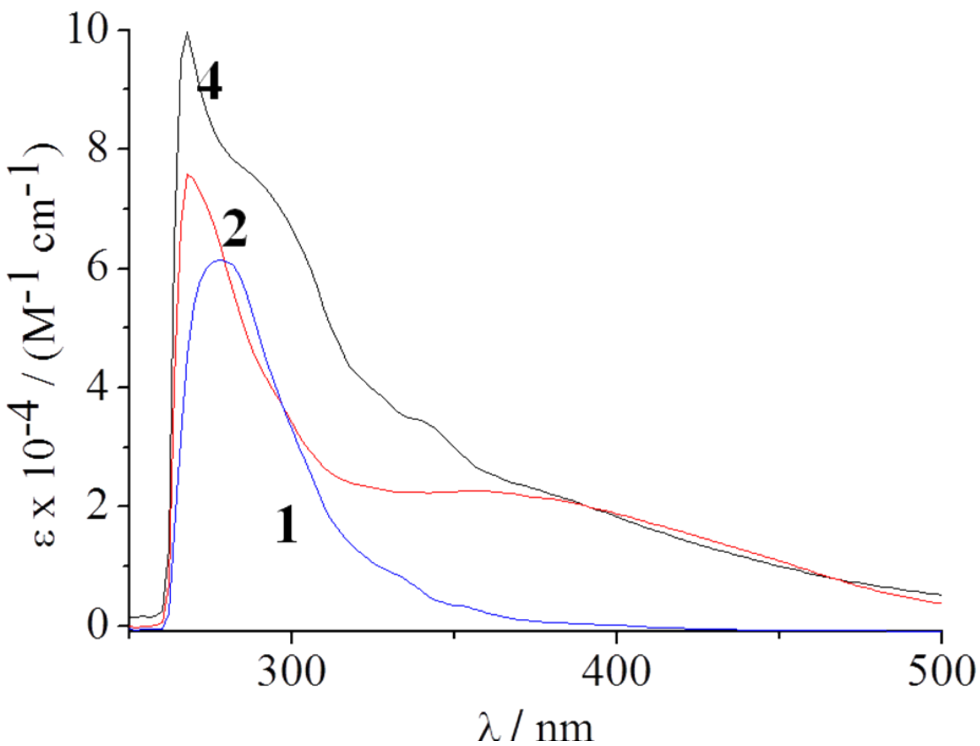

Figure S19. The absorption spectra of complexes **1**, **2**, and **4** in 5% aqueous DMF. Note that the absorption spectra of complexes **2** and **4** extend up to 500 nm.

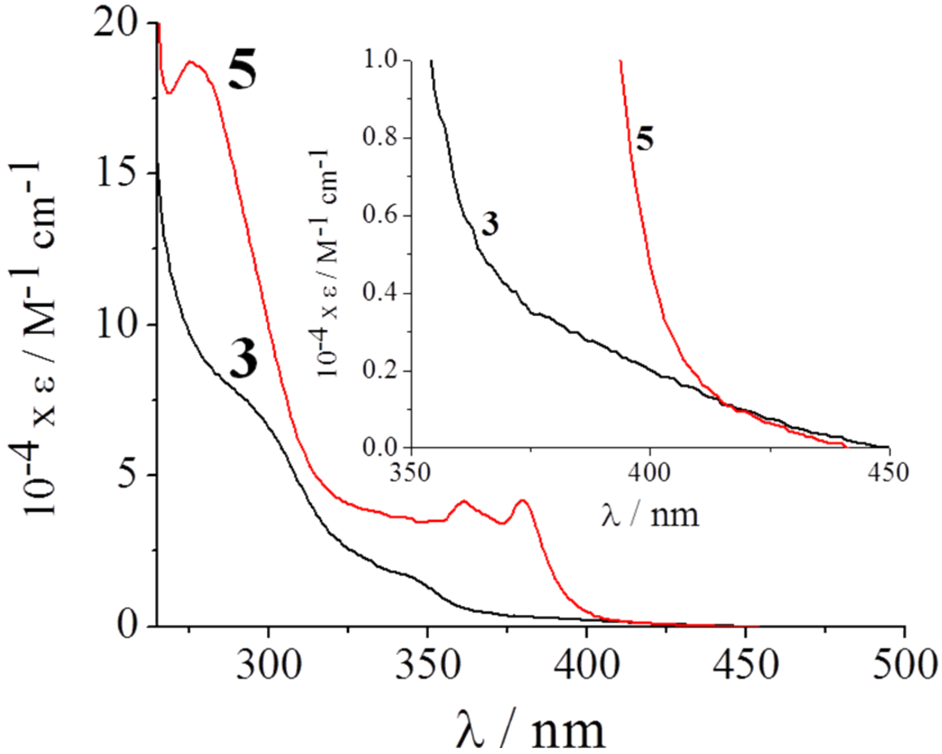

Figure S20. The electronic absorption spectra of complexes **3** and **5**. The inset depicts magnified portions of their spectra indicating that the spectral tails enter into the visible region.

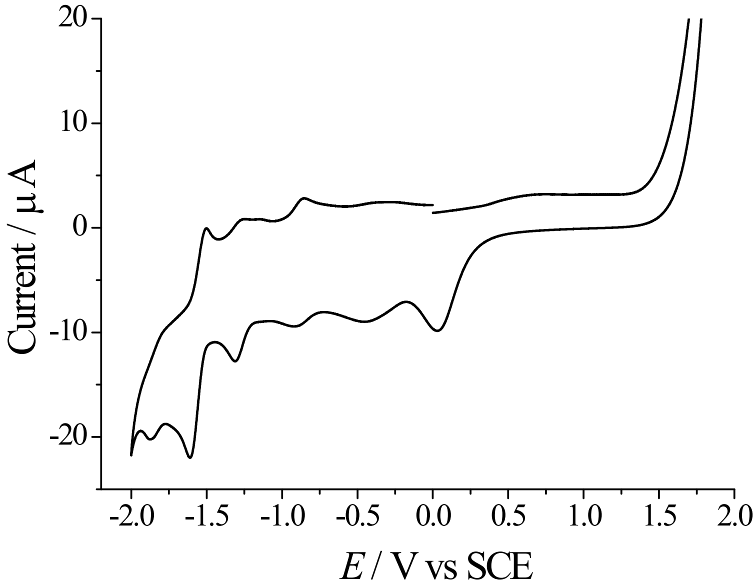

Figure S21. The cyclic voltammogram of **1** in DMF (0.1 M TBAP) showing the cathodic and anodic peaks.

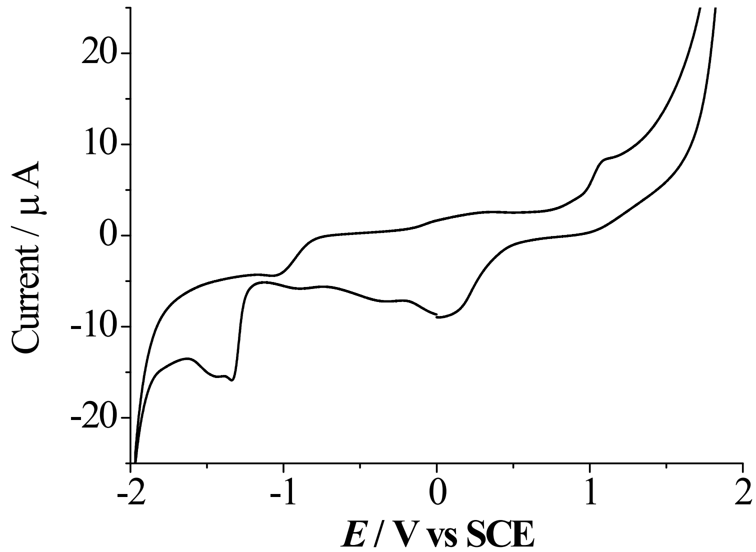

Figure S22. The cyclic voltammogram of **2** in DMF (0.1 M TBAP) showing the cathodic and anodic peaks.

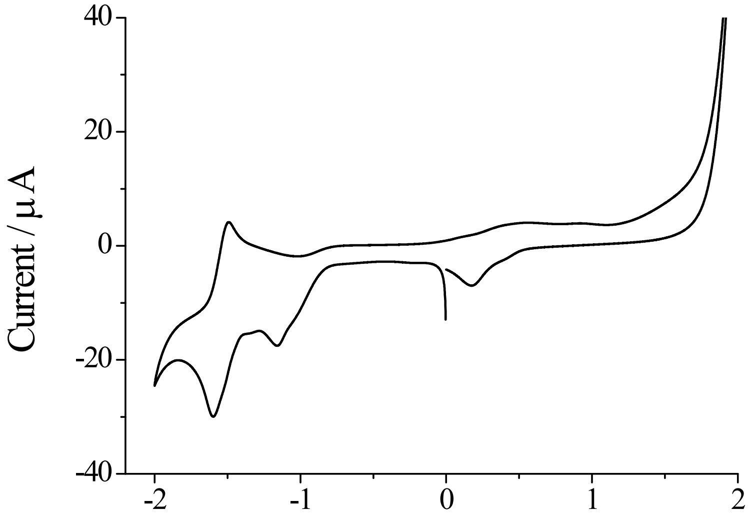

Figure S23. The cyclic voltammogram of **3** in DMF (0.1 M TBAP) showing the cathodic and anodic peaks.

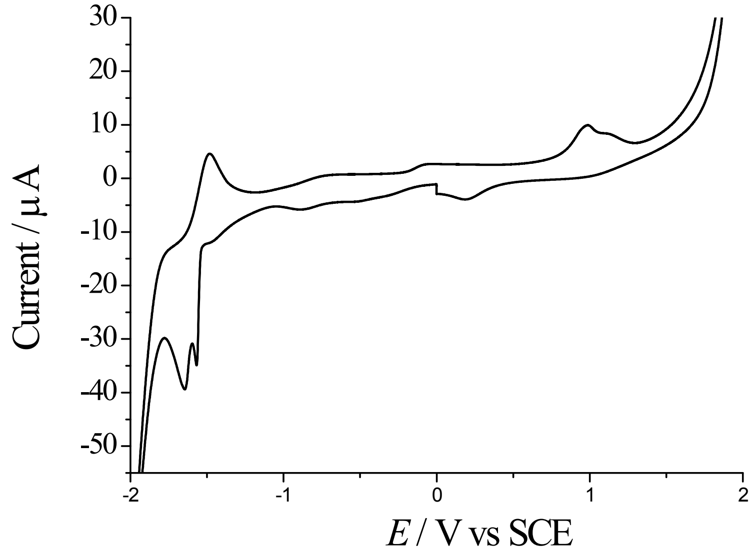

Figure S24. The cyclic voltammogram of **4** in DMF (0.1 M TBAP) showing the cathodic and anodic peaks.

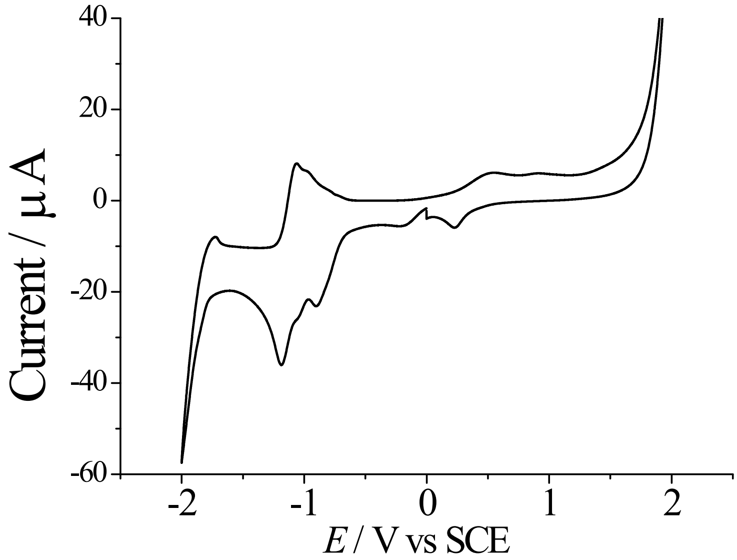

Figure S25. The cyclic voltammogram of **5** in DMF (0.1 M TBAP) showing the cathodic and anodic peaks.

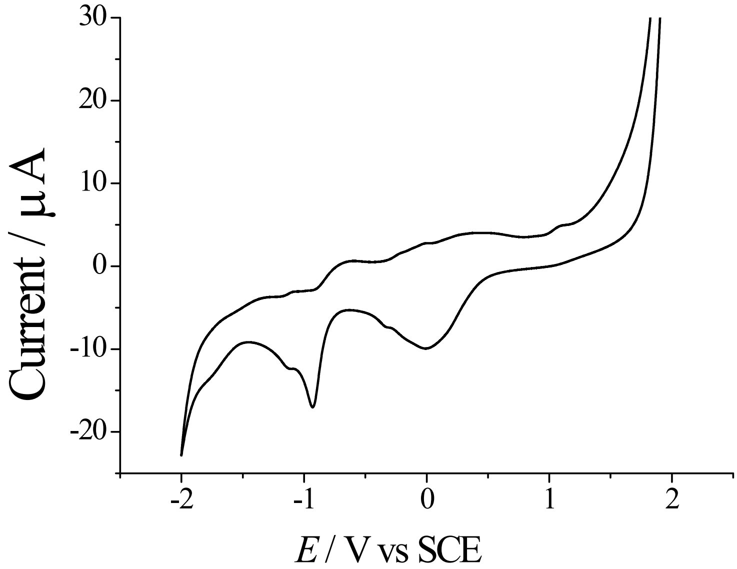

Figure S26. The cyclic voltammogram of **6** in DMF (0.1 M TBAP) showing the cathodic and anodic peaks.

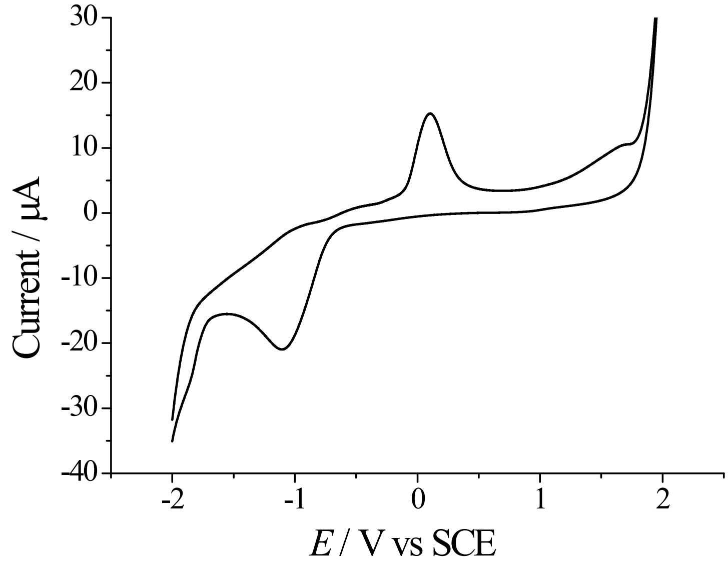

Figure S27. The cyclic voltammogram of curcumin in DMF (0.1 M TBAP) showing the cathodic and anodic peaks.

Table S1 Cathodic and anodic peak potentials (Volt vs SCE) for complexes **1-6** and the curcumin ligand.

Complex	E_{pc1}	E_{pc2}	E_{pc3}	E_{pa1}	E_{pa2}	E_{pa3}	E_{pa4}	E_{pa5}	E_{pa6}
1	-1.50	-1.25	-0.86	-1.87	-1.61	-1.30	-0.90	-0.43	0.03
2	-0.80	1.08	-	-1.33	0.06	-	-		
3	-1.50	-	-	-1.60	-1.15	0.18	-	-	-
4	-1.50	0.98	-	1.64	0.20	-	-	-	-
5	-1.06	0.51	-	-1.18	-0.90	0.24	-	-	-
6	-0.65	1.10	-	-0.93	0.00	-	-	-	-
Curcumin	0.11	-	-	-1.11	-	-	-	-	-

Notes:

1. E_{pc} and E_{pa} are the cathodic and anodic peak potentials, respectively.
2. The cyclic voltammograms of the dpq and dppz ligands in DMF (0.1 M TBAP) were previously reported in the literature.[39(c)]

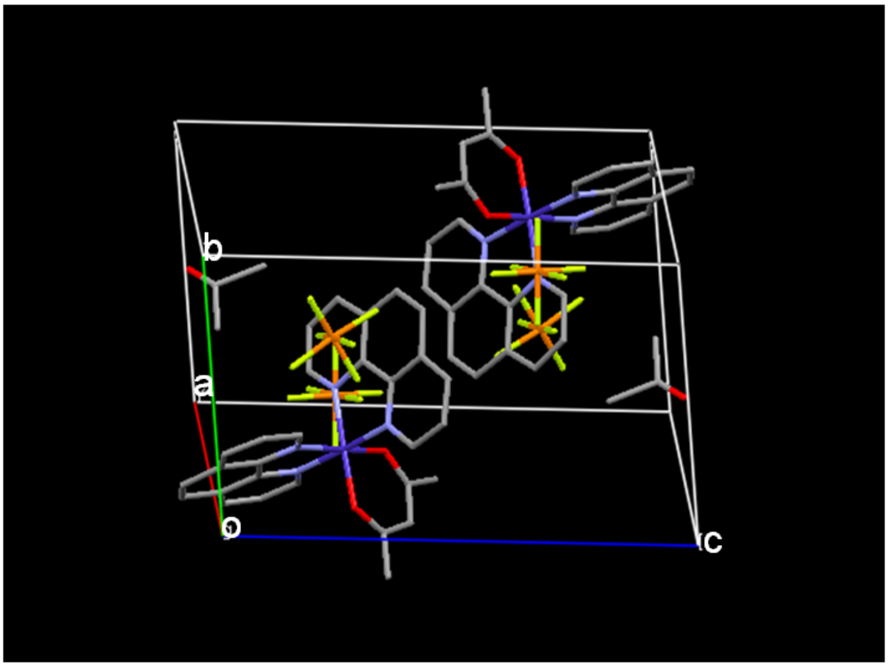

Figure S28. The unit cell packing diagram of [Co(phen)$_2$(acac)](PF$_6$)$_2$.acetone (**1a**.acetone). The complex crystallized in the Triclinic *P*-1 space group with *Z* = 2.

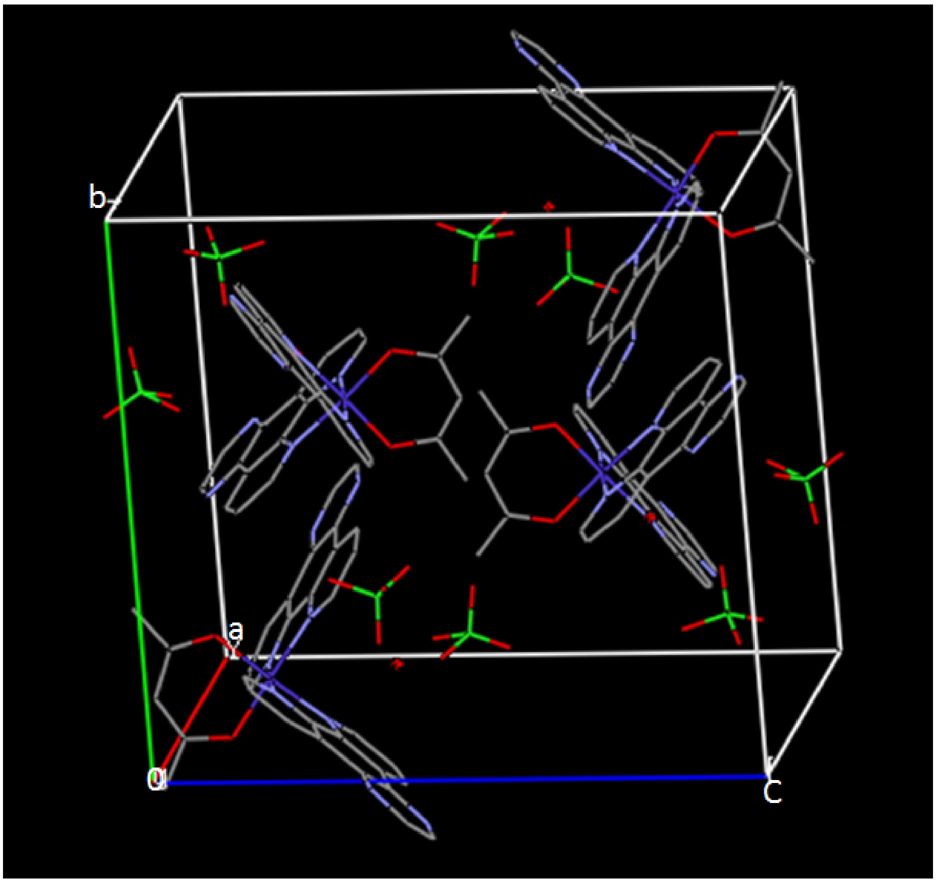

Figure S29. The unit cell packing diagram of $[Co(dpq)_2(acac)](ClO_4)_2.H_2O$ (**3**.H_2O). The complex crystallized in the monoclinic $P2_1/n$ space group with $Z = 4$.

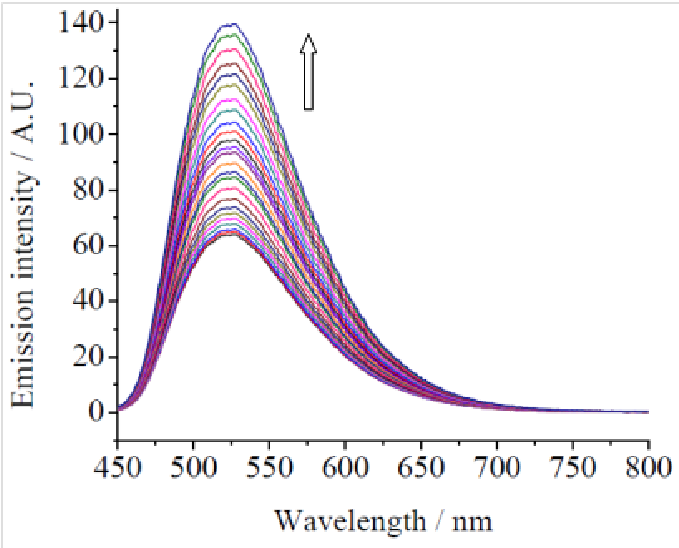

Figure S30. Emission spectral traces of **6** in a properly deaerated 5% aqueous DMF solution in the presence of ascorbic acid monitored up to 4 hours.

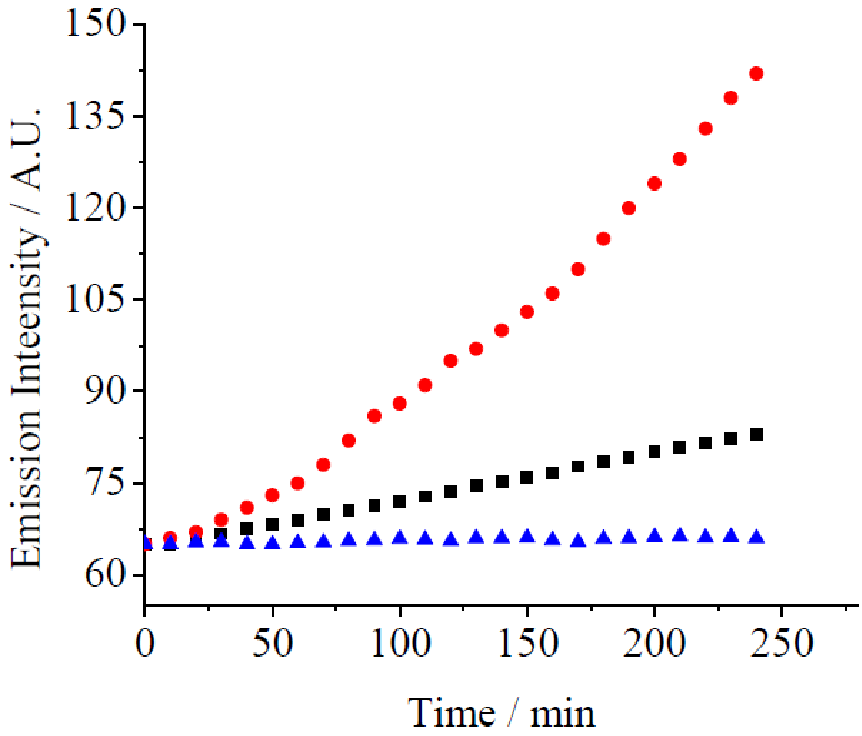

Figure S31. Time dependence of spectral emission intensity of **6** in 5% aqueous DMF in the presence of oxygen but no ascorbate (▲), in the presence of oxygen and ascorbate (■), and in the absence of oxygen but presence of ascorbate (●).

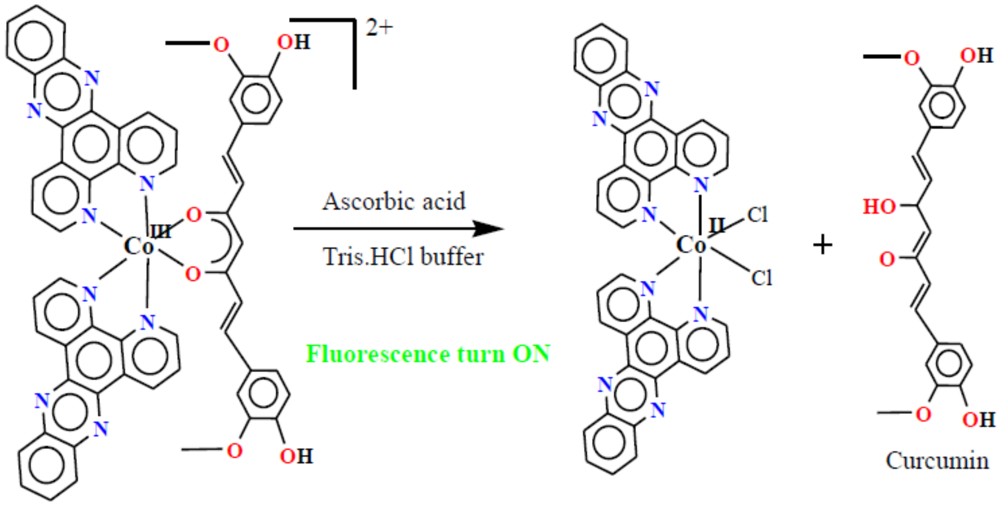

Figure S32. Reduction of Co(III) to Co(II) in $[Co(dppz)_2(cur)]^{2+}$ by ascorbic acid in the absence of oxygen and subsequent turn-on of curcumin fluorescence resulting from the release of the curcumin ligand from the complex.

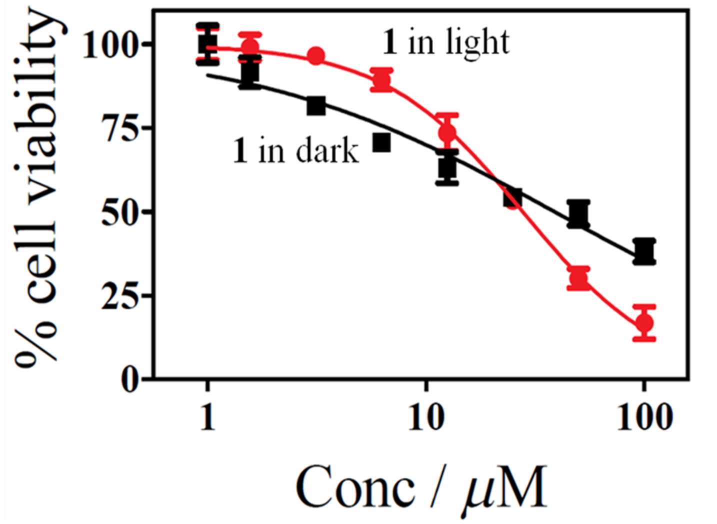

Figure S33. Cell viability plot showing the photocytotoxicity of **1** in light (red circles) and dark (black squares) in HeLa cells on 4 h incubation in dark followed by exposure to visible light (400-700 nm, 10 J cm^{-2}) for 1 h, as determined from the MTT assay.

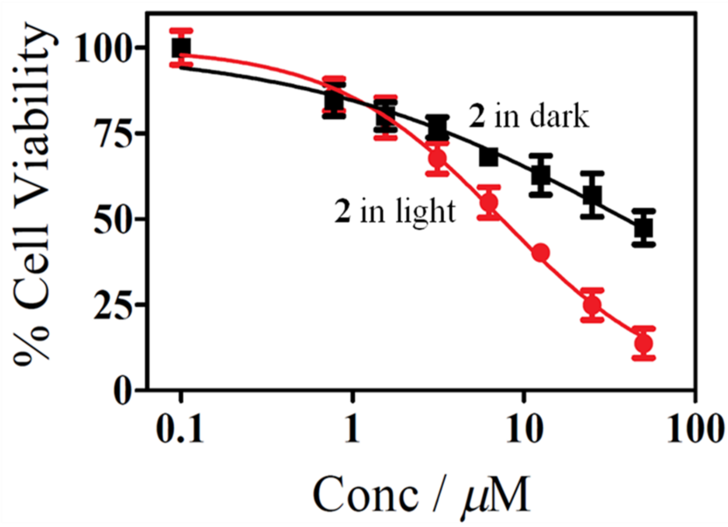

Figure S34. Cell viability plot showing the photocytotoxicity of **2** in light (red circles) and dark (black squares) in HeLa cells on 4 h incubation in dark followed by exposure to visible light (400-700 nm, 10 J cm^{-2}) for 1 h, as determined from the MTT assay.

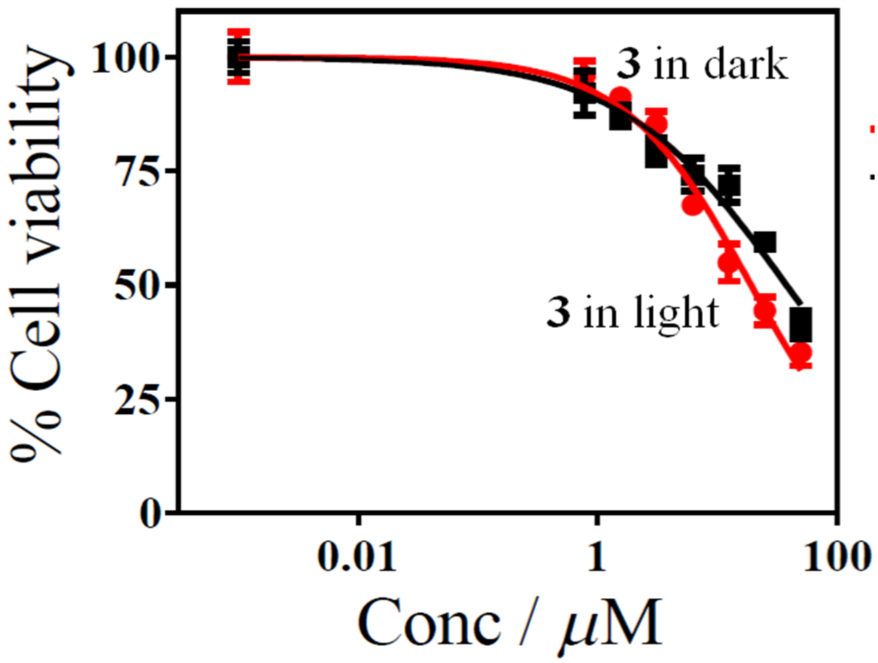

Figure S35. Cell viability plot showing the photocytotoxicity of **3** in light (red circles) and dark (black squares) in HeLa cells on 4 h incubation in dark followed by exposure to visible light (400-700 nm, 10 J cm^{-2}) for 1 h, as determined from the MTT assay.

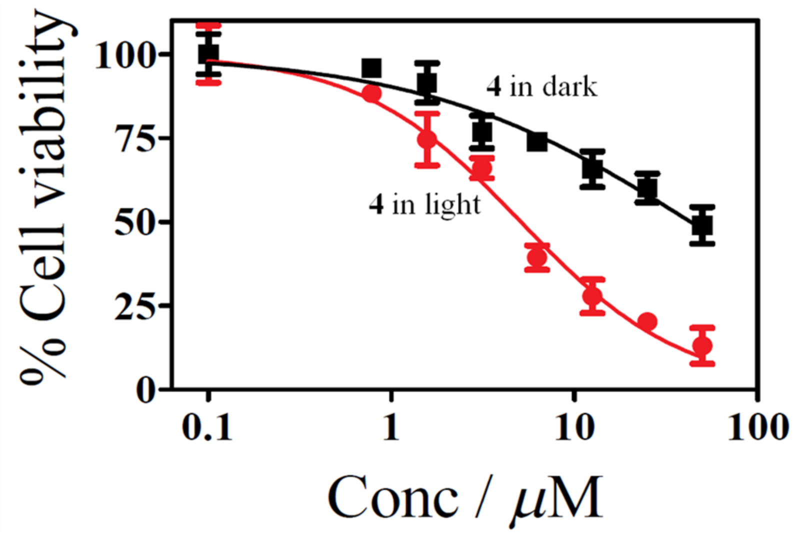

Figure S36. Cell viability plot showing the photocytotoxicity of **4** in light (red circles) and dark (black squares) in HeLa cells on 4 h incubation in dark followed by exposure to visible light (400-700 nm, 10 J cm^{-2}) for 1 h, as determined from the MTT assay.

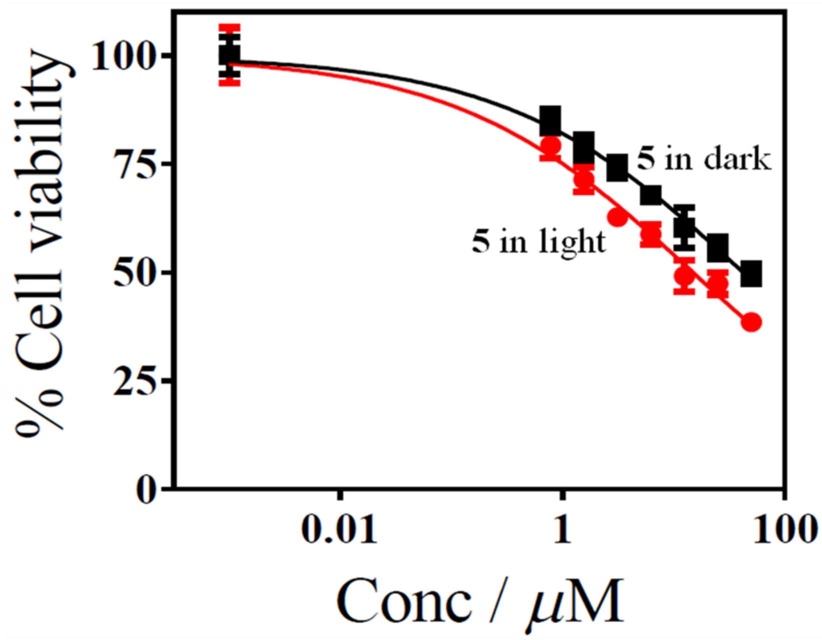

Figure S37. Cell viability plot showing the photocytotoxicity of **5** in light (red circles) and dark (black squares) in HeLa cells on 4 h incubation in dark followed by exposure to visible light (400-700 nm, 10 J cm^{-2}) for 1 h, as determined from the MTT assay.

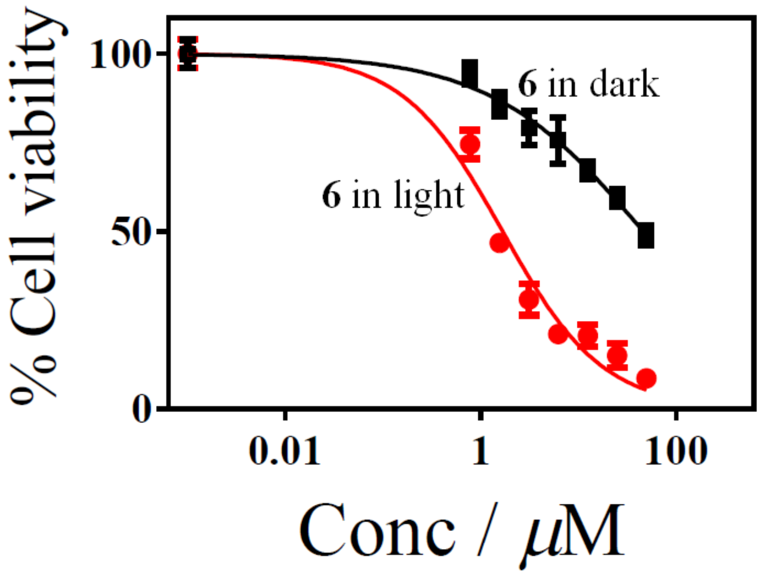

Figure S38. Cell viability plot showing the photocytotoxicity of **6** in light (red circles) and dark (black squares) in HeLa cells on 4 h incubation in dark followed by exposure to visible light (400-700 nm, 10 J cm^{-2}) for 1 h, as determined from the MTT assay.

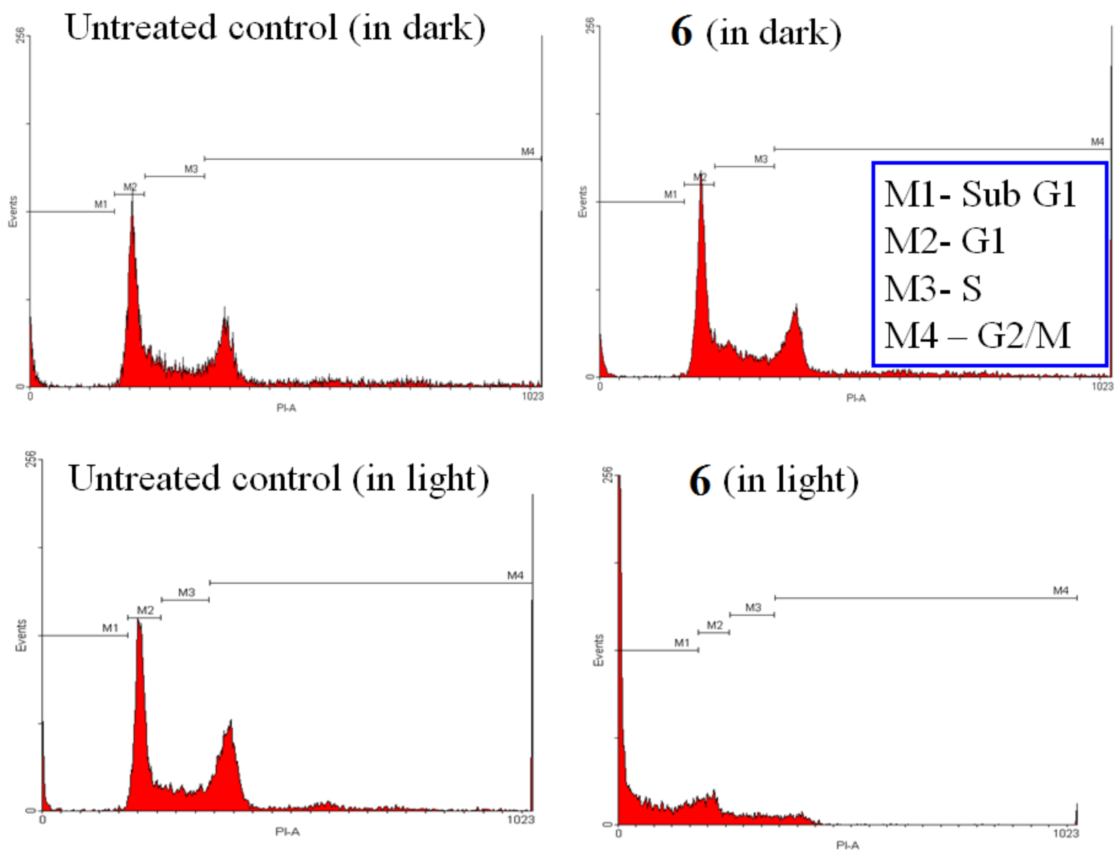

Figure S39. Flow cytometric analysis showing apoptotic cell death induced by **6**. Photo-exposure time = 1 h, light source = 400-700 nm visible light (10 J cm^{-2}), fluence rate of 2.4 mW cm^{-2}.

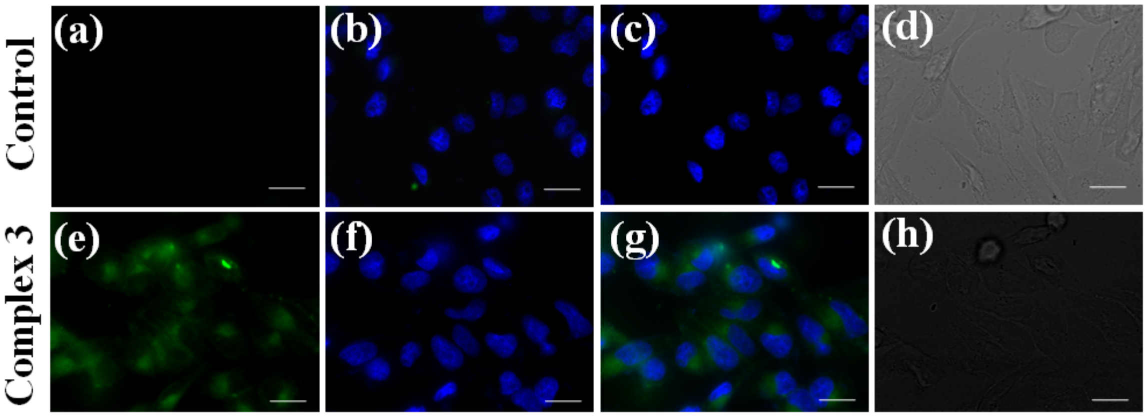

Figure S40. Fluorescence microscopic images of HeLa cells [control and treated with **6** (10 μmol)] on 2 h incubation and Hoechst 33342 dye (5 μg m^{-1}). Panel (b) is of the control. Panel (e) shows the green emission of **6.** Panels (b, f) show the blue emission of Hoechst 33342 dye which stains the nucleus. Panels (c, g) correspond to the merged images showing cytosolic localization of the complex. Panels (d, h) show the control and complex treated bright field images. Scale bar = 20 μm.

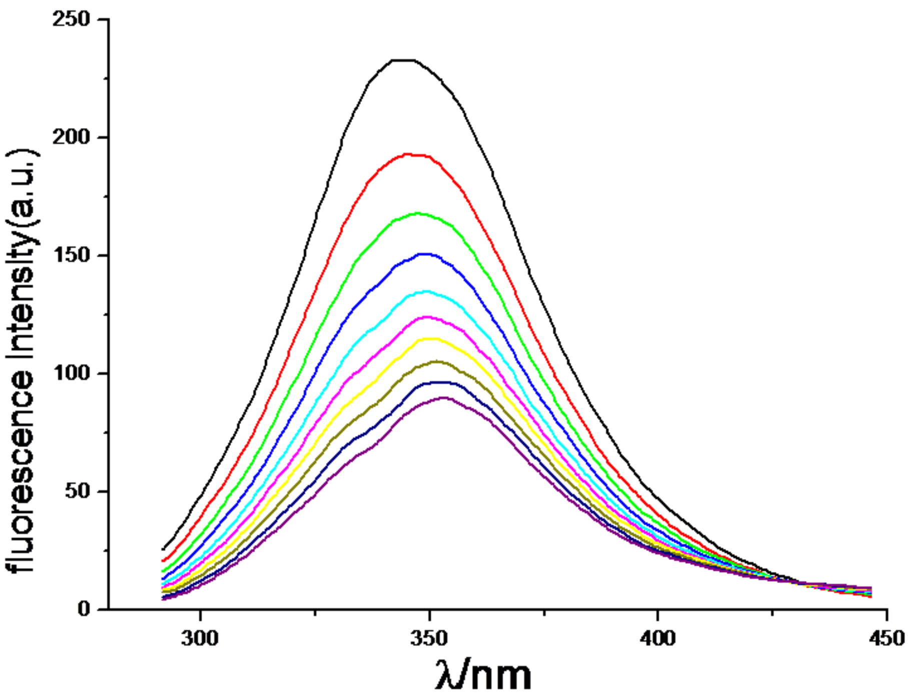

Figure S41. Emission spectral traces of human serum albumin (2 μM) in the presence of complex **3.**

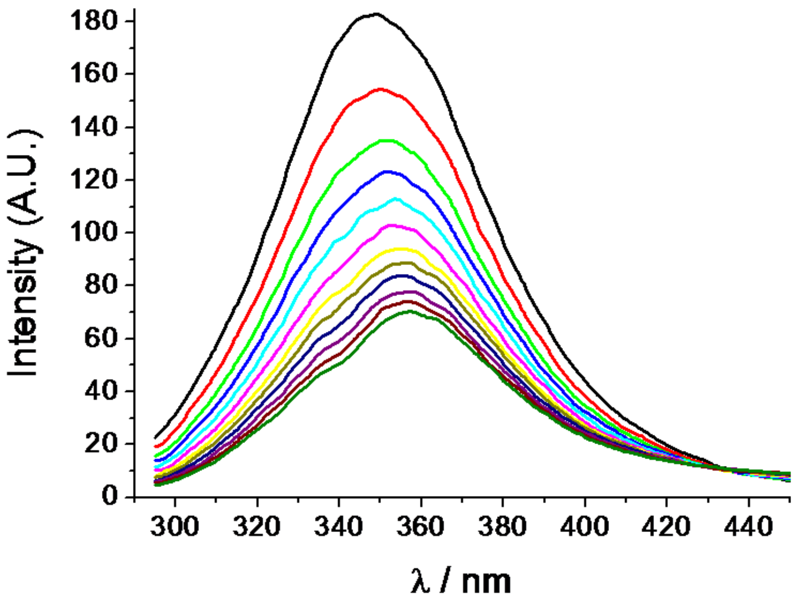

Figure S42. Emission spectral traces of human serum albumin (2 μM) in the presence of complex **5.**

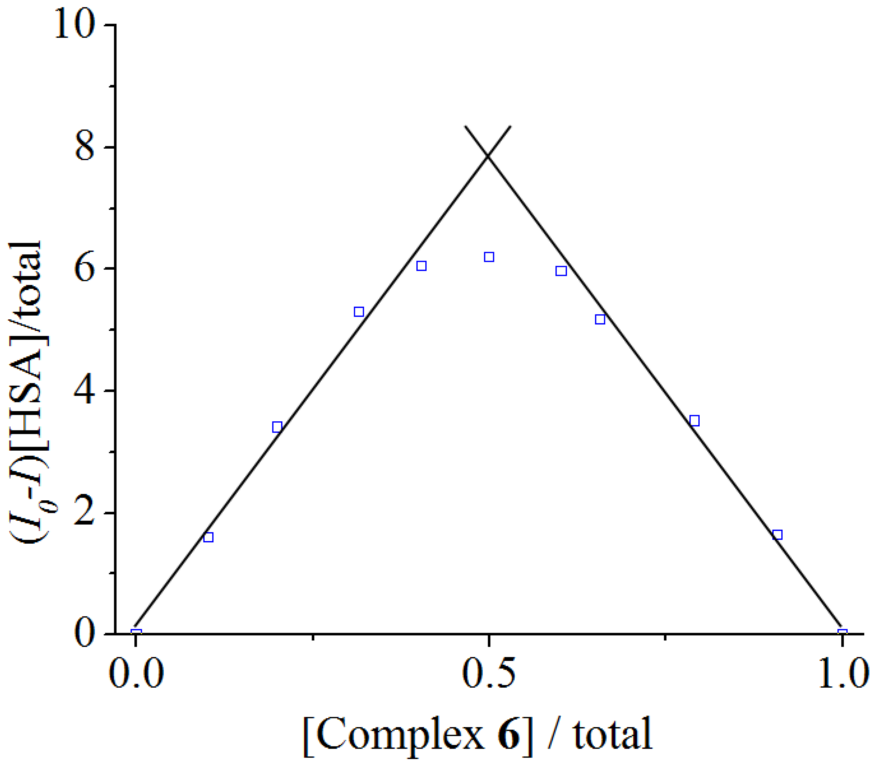

Figure S43. Job plot showing 1:1 binding stoichiometry of interaction between HSA and complex **6**.

Table S2. Computational data for the complex in **2**

Center Number	Atomic Number	Atomic Type	Coordinates (Angstroms) X	Y	Z
1	27	0	0.000042	-1.500024	-0.000065
2	8	0	-1.396327	-0.244396	-0.213053
3	8	0	1.396455	-0.244317	0.212175
4	7	0	1.423518	-2.887357	0.072275
5	7	0	-1.423497	-2.887307	-0.071720
6	7	0	0.373536	-1.505936	-1.923666
7	7	0	-0.373439	-1.504971	1.923557
8	6	0	1.448818	-2.300017	-2.235243
9	6	0	1.909971	-3.569945	1.121677
10	1	0	1.436037	-3.418158	2.083387
11	6	0	2.011092	-3.050954	-1.158364
12	6	0	-0.208562	-0.768073	-2.884773
13	1	0	-1.055121	-0.159740	-2.591837
14	6	0	1.988595	-2.389366	-3.542789
15	6	0	-3.118623	-3.907839	1.384274
16	6	0	1.251491	1.089543	0.133027
17	6	0	3.118550	-3.908728	-1.383240
18	6	0	-3.617855	-4.625748	0.260041
19	1	0	-4.463945	-5.297711	0.374681
20	6	0	-1.448793	-2.298819	2.235506
21	6	0	0.271369	-0.798150	-4.219949
22	1	0	-0.222177	-0.186841	-4.967397
23	6	0	-0.000037	1.729553	-0.000125
24	1	0	-0.000093	2.813661	0.000046
25	6	0	0.208717	-0.766721	2.884334
26	1	0	1.055383	-0.158652	2.591171
27	6	0	3.010100	-4.455192	0.986130
28	1	0	3.366939	-4.987337	1.861119
29	6	0	-1.909994	-3.570368	-1.120794
30	1	0	-1.436038	-3.419083	-2.082571
31	6	0	-1.251516	1.089475	-0.133537
32	6	0	-2.011102	-3.050253	1.158992
33	6	0	-1.988590	-2.387501	3.543090
34	6	0	3.617741	-4.626124	-0.258662
35	1	0	4.463780	-5.298206	-0.372981
36	6	0	3.120771	-3.263083	-3.757649
37	1	0	3.541239	-3.336249	-4.756855
38	6	0	1.364566	-1.600413	-4.552588
39	1	0	1.740447	-1.625269	-5.571762
40	6	0	-3.661838	-3.991844	2.722177
41	1	0	-4.511321	-4.645801	2.899255
42	6	0	-1.364525	-1.598101	4.552517
43	1	0	-1.740437	-1.622426	5.571694
44	6	0	-3.010190	-4.455465	-0.984828
45	1	0	-3.367061	-4.988008	-1.859562
46	6	0	-0.271250	-0.796101	4.219513
47	1	0	0.222337	-0.184470	4.966671
48	6	0	3.661744	-3.993421	-2.721109
49	1	0	4.511183	-4.647519	-2.897878
50	6	0	-3.120826	-3.261037	3.758365
51	1	0	-3.541303	-3.333694	4.757605
52	1	0	-2.296324	2.971927	-0.173564
53	1	0	-3.801430	0.292082	-0.406164
54	1	0	2.296133	2.972096	0.173415
55	1	0	3.801457	0.292313	0.405494
56	6	0	-2.452271	1.897846	-0.224486
57	6	0	-3.716343	1.378306	-0.360065
58	6	0	2.452190	1.898020	0.224122
59	6	0	3.716302	1.378541	0.359599
60	6	0	-4.961895	2.121677	-0.446443
61	6	0	-5.020597	3.539530	-0.387524
62	6	0	-6.179036	1.404983	-0.597363
63	6	0	-6.231734	4.237153	-0.457868
64	1	0	-4.125566	4.142855	-0.276299
65	6	0	-7.398795	2.084096	-0.670283
66	1	0	-6.164335	0.319165	-0.653543
67	6	0	-7.443348	3.491212	-0.587260
68	1	0	-8.328362	1.527738	-0.776838

69	6	0	4.961835	2.121949	0.446059
70	6	0	5.020496	3.539773	0.387236
71	6	0	6.178979	1.405257	0.597077
72	6	0	6.231631	4.237478	0.457646
73	1	0	4.125446	4.143093	0.276110
74	6	0	7.398702	2.084415	0.670024
75	1	0	6.164291	0.319444	0.653302
76	6	0	7.443214	3.491536	0.586977
77	1	0	8.328292	1.528103	0.776625
78	8	0	8.635555	4.198409	0.605323
79	1	0	9.427167	3.625067	0.673599
80	8	0	6.147424	5.609529	0.312607
81	8	0	-8.635611	4.198113	-0.605596
82	1	0	-9.427271	3.624834	-0.673721
83	8	0	-6.147839	5.609229	-0.312547
84	6	0	-7.067338	6.532958	-1.007804
85	1	0	-8.066055	6.486763	-0.572145
86	1	0	-6.620814	7.517520	-0.858107
87	1	0	-7.111305	6.296229	-2.077773
88	6	0	7.067974	6.533484	1.006093
89	1	0	8.065926	6.487482	0.568657
90	1	0	6.620957	7.517927	0.857109
91	1	0	7.113986	6.296876	2.075999

Table S3. Computational data for the complex in **4**

Center Number	Atomic Number	Atomic Type	Coordinates (Angstroms) X	Y	Z
1	27	0	0.000011	-0.998711	0.000022
2	8	0	-1.351279	0.257181	-0.408879
3	8	0	1.351298	0.257200	0.408863
4	7	0	1.401029	-2.382413	0.273333
5	7	0	-1.401011	-2.382426	-0.273198
6	7	0	0.639490	-1.010196	-1.851232
7	7	0	-0.639480	-1.010068	1.851279
8	6	0	1.745964	-1.800462	-2.013716
9	6	0	1.734020	-3.057918	1.389844
10	1	0	1.126709	-2.898317	2.271789
11	6	0	2.157152	-2.553024	-0.856432
12	6	0	0.188244	-0.274073	-2.886394
13	1	0	-0.692073	0.330726	-2.709583
14	6	0	2.445474	-1.887278	-3.234308
15	6	0	-3.276968	-3.409617	0.907018
16	6	0	1.215976	1.591781	0.323705
17	6	0	3.276905	-3.409780	-0.906855
18	6	0	-3.618362	-4.120094	-0.271104
19	1	0	-4.475158	-4.785518	-0.256507
20	6	0	-1.745995	-1.800270	2.013792
21	6	0	0.840944	-0.306273	-4.141687
22	1	0	0.452302	0.301319	-4.951399
23	6	0	0.000043	2.231822	-0.000146
24	1	0	0.000054	3.315948	-0.000211
25	6	0	-0.188254	-0.273854	2.886384
26	1	0	0.692095	0.330893	2.709547
27	6	0	2.839320	-3.940051	1.418981
28	1	0	3.069917	-4.465819	2.338993
29	6	0	-1.733995	-3.058016	-1.389660
30	1	0	-1.126648	-2.898525	-2.271599
31	6	0	-1.215921	1.591777	-0.323874
32	6	0	-2.157179	-2.552910	0.856560
33	6	0	-2.445553	-1.886946	3.234366
34	6	0	3.618307	-4.120169	0.271319
35	1	0	4.475075	-4.785631	0.256753
36	6	0	1.972340	-1.109374	-4.322164
37	1	0	2.498109	-1.154507	-5.270169
38	6	0	-1.972436	-1.108950	4.322166
39	1	0	-2.498243	-1.153973	5.270154
40	6	0	-2.839330	-3.940108	-1.418756
41	1	0	-3.069914	-4.465949	-2.338729
42	6	0	-0.841006	-0.305905	4.141654
43	1	0	-0.452380	0.301760	4.951319
44	1	0	-2.237452	3.473684	-0.556965
45	1	0	-3.687256	0.787978	-0.988695
46	1	0	2.237503	3.473701	0.556722
47	1	0	3.687310	0.788011	0.988521
48	6	0	-2.384765	2.398905	-0.617192
49	6	0	-3.609986	1.875125	-0.950264
50	6	0	2.384821	2.398924	0.616996
51	6	0	3.610027	1.875158	0.950112
52	6	0	-4.823042	2.613610	-1.257065
53	6	0	-4.885275	4.032511	-1.254525
54	6	0	-6.002815	1.890211	-1.577776
55	6	0	-6.067156	4.725329	-1.540366
56	1	0	-4.016651	4.640702	-1.024001
57	6	0	-7.193274	2.564443	-1.864852
58	1	0	-5.982958	0.803186	-1.596743
59	6	0	-7.245605	3.973425	-1.835458
60	1	0	-8.096141	2.003266	-2.099236
61	6	0	4.823073	2.613646	1.256944
62	6	0	4.885286	4.032537	1.254438
63	6	0	6.002837	1.890243	1.577692
64	6	0	6.067155	4.725380	1.540339
65	1	0	4.016652	4.640723	1.023935
66	6	0	7.193275	2.564491	1.864816
67	1	0	5.982986	0.803219	1.596655
68	6	0	7.245595	3.973470	1.835437

69	1	0	8.096138	2.003323	2.099235
70	8	0	8.417407	4.677313	2.066389
71	1	0	9.190496	4.100241	2.237670
72	8	0	6.001996	6.101749	1.431674
73	8	0	-8.417425	4.677258	-2.066288
74	1	0	-9.190513	4.100183	-2.237554
75	8	0	-6.002172	6.101718	-1.431510
76	6	0	-6.797597	6.998340	-2.294829
77	1	0	-7.851264	6.971818	-2.014554
78	1	0	-6.371001	7.987293	-2.118293
79	1	0	-6.680849	6.718405	-3.348745
80	6	0	6.798412	6.998504	2.293912
81	1	0	7.851560	6.972872	2.011585
82	1	0	6.370771	7.987236	2.118657
83	1	0	6.683968	6.717993	3.347916
84	6	0	-3.610479	-2.766449	3.306361
85	6	0	-4.018937	-3.514364	2.162365
86	6	0	-5.360329	-3.673592	4.524443
87	6	0	-5.769978	-4.419721	3.380521
88	1	0	-5.901941	-3.745285	5.461837
89	1	0	-6.633070	-5.075934	3.421153
90	6	0	4.018836	-3.514657	-2.162212
91	6	0	3.610361	-2.766837	-3.306265
92	6	0	5.769786	-4.420207	-3.380356
93	6	0	5.360139	-3.674148	-4.524325
94	1	0	6.632854	-5.076453	-3.420959
95	1	0	5.901717	-3.745943	-5.461730
96	7	0	-4.293697	-2.857174	4.488096
97	7	0	-5.107497	-4.341577	2.214041
98	7	0	5.107351	-4.341931	-2.213860
99	7	0	4.293539	-2.857686	-4.488013

Table S4. Computational data for the complex in **6**

Center Number	Atomic Number	Atomic Type	Coordinates (Angstroms) X	Y	Z
1	27	0	0.000050	-0.519657	-0.000022
2	8	0	1.222663	0.739603	0.708130
3	8	0	-1.222604	0.739472	-0.708344
4	7	0	-1.292684	-1.900343	-0.595105
5	7	0	1.292826	-1.900235	0.595222
6	7	0	-1.059469	-0.530202	1.646194
7	7	0	1.059569	-0.530361	-1.646235
8	6	0	-2.175237	-1.315429	1.542110
9	6	0	-1.342779	-2.575788	-1.760378
10	1	0	-0.538970	-2.415534	-2.467403
11	6	0	-2.299096	-2.069587	0.317403
12	6	0	-0.860633	0.206384	2.758485
13	1	0	0.039907	0.806027	2.793833
14	6	0	-3.145724	-1.397754	2.559850
15	6	0	3.398542	-2.923827	-0.095803
16	6	0	-1.113534	2.071631	-0.585826
17	6	0	-3.398385	-2.923895	0.096025
18	6	0	3.442809	-3.632338	1.129843
19	1	0	4.278441	-4.296358	1.323168
20	6	0	2.175355	-1.315552	-1.542066
21	6	0	-1.792588	0.179121	3.820964
22	1	0	-1.605775	0.786036	4.700006
23	6	0	-0.000077	2.712205	-0.000104
24	1	0	-0.000134	3.796299	-0.000105
25	6	0	0.860721	0.206108	-2.758601
26	1	0	-0.039830	0.805732	-2.794006
27	6	0	-2.407961	-3.455924	-2.055231
28	1	0	-2.409736	-3.983263	-3.002847
29	6	0	1.342941	-2.575544	1.760573
30	1	0	0.539133	-2.415222	2.467584
31	6	0	1.113453	2.071750	0.585609
32	6	0	2.299235	-2.069567	-0.317274
33	6	0	3.145843	-1.397965	-2.559797
34	6	0	-3.442631	-3.632547	-1.129540
35	1	0	-4.278250	-4.296605	-1.322793
36	6	0	-2.938852	-0.619246	3.726409
37	1	0	-3.675106	-0.659789	4.522022
38	6	0	2.938956	-0.619583	-3.726438
39	1	0	3.675211	-0.660194	-4.522047
40	6	0	2.408141	-3.455627	2.055521
41	1	0	2.409932	-3.982856	3.003198
42	6	0	1.792678	0.178753	-3.821075
43	1	0	1.605855	0.785575	-4.700180
44	1	0	2.063991	3.956144	1.020389
45	1	0	3.382325	1.274652	1.774993
46	1	0	-2.064247	3.955928	-1.020639
47	1	0	-3.382320	1.274304	-1.775233
48	6	0	2.193232	2.881871	1.119497
49	6	0	3.317463	2.361202	1.710199
50	6	0	-2.193387	2.881641	-1.119733
51	6	0	-3.317560	2.360862	-1.710445
52	6	0	4.440115	3.103597	2.260094
53	6	0	4.509286	4.521918	2.245383
54	6	0	5.518659	2.385288	2.841055
55	6	0	5.605075	5.217906	2.767863
56	1	0	3.715479	5.126808	1.819379
57	6	0	6.622226	3.063241	3.368200
58	1	0	5.489463	1.298802	2.874109
59	6	0	6.686908	4.471094	3.325755
60	1	0	7.449378	2.504911	3.803168
61	6	0	-4.440277	3.103149	-2.260352
62	6	0	-4.509579	4.521464	-2.245648
63	6	0	-5.518753	2.384738	-2.841313
64	6	0	-5.605431	5.217347	-2.768135
65	1	0	-3.715829	5.126429	-1.819645
66	6	0	-6.622381	3.062585	-3.368465
67	1	0	-5.489454	1.298255	-2.874363
68	6	0	-6.687194	4.470433	-3.326025

69	1	0	-7.449480	2.504177	-3.803434
70	8	0	-7.784967	5.178107	-3.792946
71	1	0	-8.499188	4.602853	-4.137735
72	8	0	-5.577928	6.592373	-2.619621
73	8	0	7.784618	5.178871	3.792671
74	1	0	8.498885	4.603683	4.137478
75	8	0	5.577432	6.592928	2.619348
76	6	0	6.137117	7.500738	3.640971
77	1	0	7.226766	7.454303	3.646128
78	1	0	5.789582	8.490508	3.339656
79	1	0	5.743883	7.248325	4.633472
80	6	0	-6.137608	7.500117	-3.641306
81	1	0	-7.227251	7.453543	-3.646594
82	1	0	-5.790236	8.489930	-3.339947
83	1	0	-5.744220	7.247757	-4.633761
84	6	0	4.305325	-2.272837	-2.359102
85	6	0	4.430512	-3.032357	-1.132574
86	6	0	6.309998	-3.173905	-3.126392
87	6	0	6.436171	-3.937305	-1.893012
88	6	0	7.318860	-3.287497	-4.128648
89	6	0	7.566204	-4.787561	-1.705970
90	6	0	8.405484	-4.123060	-3.915740
91	1	0	7.207395	-2.710325	-5.040689
92	6	0	8.529579	-4.875895	-2.700159
93	1	0	7.641886	-5.349444	-0.780782
94	1	0	9.177205	-4.214635	-4.674610
95	1	0	9.392323	-5.521807	-2.565014
96	6	0	-4.305188	-2.272671	2.359248
97	6	0	-4.430358	-3.032327	1.132803
98	6	0	-6.309847	-3.173691	3.126630
99	6	0	-6.436004	-3.937227	1.893333
100	6	0	-7.318711	-3.287191	4.128896
101	6	0	-7.566022	-4.787521	1.706379
102	6	0	-8.405321	-4.122794	3.916074
103	1	0	-7.207258	-2.709919	5.040875
104	6	0	-8.529399	-4.875763	2.700574
105	1	0	-7.641693	-5.349505	0.781252
106	1	0	-9.177043	-4.214300	4.674952
107	1	0	-9.392133	-5.521704	2.565497
108	7	0	-5.233573	-2.351555	3.329474
109	7	0	-5.480319	-3.845027	0.916755
110	7	0	5.233709	-2.351811	-3.329322
111	7	0	5.480488	-3.845015	-0.916441